

Ecosystem response in temperature fronts in the northeastern Arabian Sea

V.V.S.S. Sarma¹, D. V. Desai², J.S. Patil², L. Khandeparker², S.G. Aparna², D. Shankar², Selrina D'Souza², H.B. Dalabehera¹, J. Mukherjee¹, P. Sudharani¹, A.C. Anil²

¹CSIR-National Institute of Oceanography, Regional Centre, 176 Lawsons Bay Colony, Visakhapatnam, India

²CSIR-National Institute of Oceanography, Dona Paula, Goa, India

Corresponding author (sarmav@nio.org)

Abstract

Productivity is low in tropical waters outside the traditional upwelling regimes, making temperature fronts a potential marker of fish. To test the hypothesis that all temperature fronts harbour high concentrations of nutrients and phytoplankton biomass, several fronts were sampled during winter 2014 in the northeastern Arabian Sea (NEAS). The data suggest that all the sampled temperature fronts are active biological spots owing to injection of subsurface nutrients into the surface layer. The plankton response, however, varied, with enhanced zooplankton biomass (total bacterial counts) in the shelf (open-ocean) fronts, suggesting that classical (microbial) food webs are active. The plankton response depended on the age of the front, and, more importantly, the initial or background conditions under which a front forms. Determination of the initial conditions for a front is complicated owing to advection by the mean current and mesoscale eddies and this advection itself modulates the background conditions. An increase in integrated Chlorophyll-*a* (Chl-*a*), but not surface Chl-*a*, was observed in both shelf and open-ocean fronts, suggesting that depth-integrated Chl-*a* is likely to be a better marker of potential fishery zones (PFZs). This study suggests that the PFZ advisories may be improved by including depth-integrated Chl-*a*, the age of the front, and background conditions in the procedure.

Keywords: Frontal systems, vertical mixing, zooplankton, Indian Ocean, boundary currents.

1. Introduction

Fronts are ubiquitous dynamical features of the ocean's circulation and are known to be sites of high biological productivity (Yoder et al., 1994). Vigorous vertical motion occurs in the frontal zones (Pollard and Regier, 1990; Rudnick and Luyten, 1996) resulting in the supply of inorganic nutrients from below the mixed layer (ML), implying that ocean fronts can support enhanced phytoplankton growth relative to the surroundings (Franks, 1992; Fiala et al., 1994; Pitcher et al. 1998; Basterretxea and Aristegui, 2000; Jacquet et al., 2002; Brown et al., 2008; Munk et al., 2003; McManus and Woodson, 2012). Larger predators respond to planktonic aggregations in fronts, creating biological hotspots (Owen, 1981; Polovina et al., 2001; Woodson and McManus, 2007; Benoit-Bird, 2009). Hence, fronts contribute significantly to the regional ecosystem productivity and also to the carbon and nitrogen cycling, making it important for understanding the underlying mechanisms associated with potential for fisheries (Bjorkstedt et al. 2002) and cycling of carbon and nitrogen (Chen et al., 1983; Liu et al., 2003; Zhao et al., 1985; Lu et al., 2010; Li et al., 2000).

Fronts are generally identified using temperature, particularly sea surface temperature (SST), because it can be mapped using satellites (Franks, 1992; Solanki et al., 2000; 2001; Clayton et al., 2014). Temperature fronts form between warm and cold waters (Pingree et al., 1979; Belkin et al., 2009; Schneider and Qiu, 2015). Since a higher horizontal temperature gradient is usually associated with stronger vertical velocities and mixing (Klein and Lapeyre, 2009; Schneider and Qiu, 2015), the more productive fronts tend to occur in the mid-latitudes and polar regions (Petrusevics et al., 2011; Polovina et al., 2015). Examples from polar region include frontal zones in the Bering Sea (Schneider et al., 1990; Coyle and Cooney, 1993; Decker and Hunt, 1996; Brodeur et al., 1997; Flint et al., 2002). Much more attention, however, has been devoted to frontal systems in the subtropics, where fronts have been studied, for example, in the regime of the Florida Current and the Gulf Stream (Belkin et al., 2009), the California Current System (for eg. Miller et al., 1999), western English Channel, the Armorican Shelf (Jordan and Joint, 1984; Borges and Frankignoulle, 2003; Suykens et al., 2010), the Kuroshio (Nagai et al., 2012; Clayton et al., 2014), and the Southern Ocean (Boutin et al., 2008; Petrusevics et al., 2011; Resplandy et al., 2014). These studies examined the vertical mixing, plankton distribution, juvenile fish distribution, and the carbon and nitrogen fixation associated with the fronts. Stukel et al. (2011) noted that subduction at fronts is responsible for the massive imbalance of new versus export production that arises when only contemporaneous processes in homogeneous water parcels are considered. Taylor and Ferrari (2011) suggested that fronts play a significant role in the generally oligotrophic subtropical waters by drawing more

nutrients into the euphotic zone, triggering patchy blooms (Lévy et al., 2001; McGillicuddy et al., 2007; Mahadevan et al., 2008).

The tropical waters are known to be even more oligotrophic than the subtropical waters, leading to lower productivity outside the traditional upwelling regimes (Barber et al., 2001; Behrenfeld and Falkowski, 1997). This lower productivity makes fronts a potentially useful marker of fish in the tropics, including the seas around India. This hypothesis, that the fronts in tropical waters would be richer in fish, forms the basis for the studies (Solanki et al., 1998, 2000, 2003, 2010) that led to the advisories on potential fishery zones (PFZs) issued by the Indian National Centre for Ocean Information Systems (INCOIS) (<http://www.incois.gov.in>).

Unlike in the subtropical or polar waters, the horizontal temperature or SST gradients associated with tropical fronts are much weaker, and the PFZ advisories therefore tend to use satellite Chl-*a* data in addition to satellite SST data for mapping PFZs (Solanki et al., 1998, 2000, 2003, 2010). Fishery studies carried out to evaluate PFZ advisories suggest an increase in the fish catch in the designated zone compared to, say, 10-50 km away from it (see, for example, Nammalwar et al., 2013). None of these studies, however, allows for the different background conditions under which a front evolves; instead, they proceed directly from the SST and Chl-*a* to the fish.

An intricate web of physical and biogeochemical processes must provide the connection between the SST, which is a physical variable, or even satellite Chl-*a*, and the higher trophic levels. In order to study the ecosystem dynamics of these frontal systems in the seas around India, the CSIR-National Institute of Oceanography launched an inter-disciplinary program called OCEAN FINDER in 2012. The most productive region in the Indian Exclusive Economic Zone (EEZ) is the northeastern Arabian Sea (NEAS; Figure 1) (Banse, 1968; Madhupratap et al., 1996; Bhattathiri et al., 1996; Barber et al., 2001; Shankar et al., 2015, Vijith et al., 2016). Less clouding over the NEAS during the winter monsoon (November-February) leads to more clear pixels (Obenour, 2014) and more fronts can therefore be identified in SST and Chl-*a* data. Anecdotal evidence also suggests that the PFZ advisories are popular among the fishermen from this region, leading to the first cruise under this program sampling at a high resolution across a filament and a front in the NEAS during November-December 2012 (Vipin et al., 2015; Roy et al., 2015). The CTD data were collected at a resolution of ~ 1 nautical mile in the neighbourhood of the filament and showed an increase in the Chl-*a* confined to the width of the filament (Vipin et al., 2015). Nutrient concentration (Roy et al., 2015), bacterial abundance, picophytoplankton concentration, and zooplankton abundance were also higher in the

regime of the filament compared to the more oligotrophic water to its south on this meridional transect at 69.2°E.

This transect was mapped in 2012 following the detection of the filament and front in satellite SST data. Therefore, a useful question in the context of SST fronts and PFZs is whether any such front would show a similar increase in biological activity. In order to test this hypothesis — all temperature fronts harbour higher nutrient levels, phytoplankton biomass, and productivity —, we sampled across several fronts in five transects on a cruise during 22 January to 3 February 2014 in the NEAS. This cruise was conducted during late winter, while the cruise reported by Vipin et al (2015) was conducted during early winter (November-December 2013). Hence, as a consequence of convective mixing, the waters can be expected to be more productive in the entire region (Banse, 1968; Madhupratap et al., 1996; Wiggert et al., 2002; Shankar et al., 2015). The question posed above is nevertheless valid because it is of interest to know if the fronts are more productive than the surrounding regions irrespective of the background conditions. Implications for the carbon and nitrogen cycling are obvious corollaries. The second question of interest is whether phytoplankton biomass is low in the regime of such fronts or PFZs as a consequence of the increase in fish production and grazing.

Hence, the transects were used to sample across fronts over a large part (roughly 25000 sq. km) of the NEAS, ranging from the open ocean (~68.6°E; less productive) to the inner-shelf regime (~70°E; more productive) and from ~19.5°N to 21°N as Chl-*a* increases poleward in the NEAS (Shankar et al., 2015). This paper presents the variability observed across the fronts on this cruise and an earlier paper described the inorganic carbon components in these fronts (Sarma et al., 2015). We show that fronts in general tend to be more productive than the surroundings, bacteria are the first to respond in the open ocean and zooplankton on the shelf to the physical forcing that makes nutrients available, and grazing pressure plays a role in the evolution of the ecosystem. The data suggest that the productivity associated with the ecosystem in a frontal regime depends on the age of the front and, more important, its evolution depends on the initial conditions. The most important inference drawn is that advection of the fronts by the large-scale flow leads to the increased productivity in the frontal regime being distributed over a larger region, thereby potentially contributing to an increase in the average productivity in the region.

The paper is organized as follows. We describe the materials and methods in Section 2 and present the cruise data in Section 3. Section 4 discusses the results and concludes the paper.

2. Materials and methods

The cruise, #SSK-060 on board *RV Sindhu Sankalp*, was conducted during 22 January to 3 February 2014. Since Mormugao in Goa was the port of embarkation and disembarkation, about one week, i.e., the period from 24 January to 1 February, was available for sampling. Samples were collected in seven transects, but two of them were in the much warmer, oligotrophic waters south of the NEAS and were mapped while returning to port (Sarma et al., 2015). This paper is restricted to the five transects sampled in the more productive waters of the NEAS during 24-30 January (Figure 1).

2.1. Mapping fronts and the physical sampling

SST data made available in near-real-time by INCOIS were used to identify fronts using the algorithm of Cayula and Cornillon (1992). The procedure, which uses data from four satellites, MODIS, NOAA-18, NOAA-19, and MetOp-B, has been described in detail in Vipin et al. (2015): the window size was 32 X 32 pixels and the front-detection sensitivity parameter was 0.76 (Cayula and Cornillon, 1992), but the mean temperature difference between the two populations (surface waters) on either side of a front was 0.15 °C (Vipin et al., 2015), lower than the value of 0.375 °C used in the northwest Atlantic (Ullman and Cornillon, 2000) owing to the weaker temperature gradients in the NEAS.

To determine the age of a front, a sequence of 12-hourly SST images from MeTop-B, NOAA-18, and NOAA-19 was mapped and the evolution and the movement of the fronts tracked for about 10-15 days and six times in a day depending on the availability of cloud-free SST images. The age of the front was determined based on the date on which it first appeared and the date on which it was sampled. The change in shape and size of the fronts and their movement in time and space were taken into consideration for determining the age.

CTD (conductivity-temperature-depth) casts were made at 32 stations on the five transects. The CTD used was a SeaBird 911Plus, as in Vipin et al. (2015), and the rosette was fitted with 10l Niskin bottles for collecting water samples. For consistency, we plot the CTD data at the lower vertical resolution of the bottle samples.

2.2. Biogeochemistry and primary productivity

Dissolved oxygen (DO) was measured following the Winkler titration method (Carritt and Carpenter, 1966). Nutrients (nitrate, nitrite, phosphate and silicate) were estimated using Autoanalyzer (Skalar San Plus, The Netherlands) following colorimetric procedure (Grashoff et al., 1985). About 5-10 liters of water from different depths was filtered through pre-combusted GF/F filter (0.7 µm pore

size, 47 mm diameter; Whatman) for six hours at 300° C at low vacuum and dried at 60° C for at least 24 hours. An aliquot of filter was acid fumigated for 12 hours in a desiccator to remove inorganic carbon. The particulate organic carbon (POC) and nitrogen (PN) on the filter were measured by elemental analyzer (M/S Thermo Electron, Germany) using internal reference materials of Glutamic Acid, Alanine, Marine sediments, and IAEA standards. The long-term precision of the instrument was 0.02% for both carbon and nitrogen (Sarma et al., 2012; 2015).

Phytoplankton biomass, represented as Chl-*a*, was measured using High Performance Liquid Chromatography; a detailed description of the analysis is given in Roy et al. (2015). The Fv/Fm ratios were measured *in situ* using Fast Repetition Rate Fluorometer (FRRF, Mark III, ChelSea Technologies, UK) at one meter interval. The mean ratios in the upper 50 m are used in this study.

Aliquots of 4.5 ml of the water sample were taken (n=3) for total bacterial count (TBC) analysis and fixed with 1% paraformaldehyde (final concentration) and stored at -80°C until analysis in the onshore laboratory. The samples were thawed at room temperature and stained with SYBR Green I (1:10000 final concentration, Molecular probes, USA) and incubated in the dark for 15 minutes before measurement. Flow cytometric absolute cell counting was measured using BD FACS Aria II instrument equipped with 488 nm blue laser with sheath fluid of BD FACS flow. Emitted light was collected through the filters sets 488/10 band pass (BP) for right angle light scatter (SSC) and 530/30 BP for green fluorescence. Fluorescent beads (1 µm, polysciences) were used as internal standards and for calibration of the above variables. The flow cytometric data were processed using BD FACS ARIA II software.

The primary productivity (hereafter PP) in the water at different depths in the euphotic zone was measured using enriched sodium bicarbonate (NaH¹³CO₃; 99%; Sigma Aldrich, USA) following Hama et al. (1983). About one liter of the sample was taken in Nalgene transparent bottles; 2 mM of enriched sodium bicarbonate spike was added and the spiked sample was incubated in triplicate light and dark bottles in the deck incubator under running surface seawater to control the temperature of the incubator. Samples were incubated for 24 hours and filtered through pre-combusted GF/F filters in the same manner as the POC samples.

The enrichment of the isotopic composition of the carbon was measured using elemental analyzer coupled to the isotope-ratio mass spectrometer (IRMS; Delta V Plus, Thermo Electron, Germany). The initial isotopic compositions of carbon and nitrogen were measured by filtering the sample soon after addition of spike. The computation of primary production from the concentration of POC and isotopic enrichment was done following Hama et al. (1983).

Mesozooplankton sampling was carried out by a net (100 μm) haul from 50 m to the surface. Hence, for consistency, we report all data as averages or integrals for the top 50 m even though the CTD casts were made to 200 m. Owing to the convective mixing during 226 November-January (Banse, 1968; Madhupratap et al., 1996; Shankar et al., 2015), the mixed-layer depth (MLD), defined as the depth at which the density increase from the surface 228 corresponds to a 1° C decrease in temperature (Shenoi et al., 2004, Shankar et al., 2015), exceeded 50 m at 32 of the 34 stations sampled during the cruise; of the other two stations, the bottom was shallower than 50 m at one and the ML extended to the bottom (Figure S1). Hence, the average or integral over 50 m essentially allows us to study the horizontal variation within the ML across the fronts.

3. Results

Even though the cruise was restricted to the NEAS, the area covered was large enough to permit significant spatial variation in the background conditions under which the fronts evolved on the five transects that were mapped. Therefore, the observations made on these five transects are described in this section using space, rather than time, as a marker: the transects are not described in the order in which they were sampled. The fronts were at different stages of evolution when they were sampled, adding to the heterogeneity imposed by the variations in background conditions. We describe the background conditions first, followed by a description of each of the transects, starting with two open-ocean transects in order from south to north, followed by a transect in the intermediate zone between open ocean and shelf, and then two transects that sampled across fronts on the shelf or near the coast. We end this section by discussing the processes involved.

3.1. The background conditions

In the climatology, SST decreases poleward in the NEAS during the winter monsoon (Chatterjee et al., 2012; Shankar et al., 2015) and this expectation from climatology was true for the SST averaged over 24-30 January 2014, the sampling week (Figure 1). The SST also decreased towards the coast as well as away from the continental slope. This peaking of the SST on the continental slope and outer shelf is consistent with the expectation of poleward advection of warmer (and fresher) surface water by the West India Coastal Current (WICC), which is the boundary current in the eastern Arabian Sea; the WICC is known to flow poleward during the winter monsoon (Shetye et al., 1991; McCreary et al., 1993; Shankar and Shetye, 1997; Amol et al., 2014; Shankar et al., 2015). The climatology also suggests a poleward increase in the MLD and Chl-*a* within the NEAS (Figure 1; Shankar et al., 2015). An increase in Chl-*a* is also expected as one moves from the open ocean onto

the more productive continental shelf (Figure 1). These spatial differences in the background conditions are expected to be maintained as the season progresses (Bhattathiri et al., 1996; Barber et al., 2001). Since the WICC flows poleward, the fronts are also likely to be advected poleward by this mean background flow. Unfortunately, the data on nutrients (Wyrski, 1971; Garcia et al., 2014) are too sparse in the NEAS to permit any reliable inference regarding their spatio-temporal distribution (Vijith et al., 2016); hence, we do not show these figures, but refer the reader to Vijith et al. (2016; their Figures 3 and S1).

Superimposed on this gradual seasonal cycle, which may be assumed to stay roughly constant over the sampling duration of the order of a week, is variability at shorter time scales. The SST in the NEAS responds to the intraseasonal changes in the air-sea fluxes even though the MLD changes more slowly in time (Shankar et al., 2015). This intraseasonal variability, whose time scale can range from a few days to ~90 days, need not show the same spatial variation as the seasonal cycle, and can therefore distort the more gradual and fairly monotonic spatial variations associated with the seasonal cycle. Hence, the immediate background conditions under which a front forms may deviate from the climatological expectation.

Therefore, it is essential to describe the background conditions to appreciate the changes that take place in these fronts. Defining the background conditions is tricky, however, because there are multiple possibilities. Our first definition of the background uses the immediate surroundings of the fronts, which would be represented by the non-frontal (NF) regime in a transect that samples across a front. In this definition, the stations marked as frontal stations in Figs. 2-6 are used for estimating the frontal average and all other stations on the transect for estimating the NF average. Since a transect takes about a day to cover, the dynamic nature of fronts — that they are advected — implies that the front being sampled or some other front may have passed through the NF regime of the transect in the near past. With the limited data, particularly chemical and biological data, available for studying these dynamic ecosystems, this limitation is unavoidable. Our second definition of the background conditions is obtained by including all the stations, including those within the frontal regime in Figs. 2-6, in the computation of the average for the NF regime. Though the difference between the frontal and NF regimes tends to be less for the second definition compared to the first (Table 1), these two definitions of the background are similar because they are local: in both cases, the average is computed separately over each transect and both definitions of the background conditions are therefore limited in their geographical coverage. Our third definition of the background conditions averages over all stations (both frontal and NF regimes) for all five transects:

this average, which is a single number representing the average conditions in the region as determined by the *in situ* observations, is more representative of the average background conditions across the NEAS than the first two definitions. Yet, it too has its drawbacks owing to the heterogeneity of the transects: one does expect different conditions on the slope or in the open ocean and on the shelf, and the limited data, restricted to just five transects, imply that all these averages have to be interpreted with caution. For the SST, we can use yet another definition because we can estimate the average SST over the domain shown in Fig. 1 during 24-30 January 2014. The background SST, according to this definition, was 24.86°C and ranged from 21.22°C (minimum) to 26.79°C (maximum); the background SST estimated according to the third definition (average over all five transects), was 25.02°C (Table 1).

Unless otherwise specified, we consider the transect average (second definition) to be representative of the background conditions in which a front evolves and it is evident from the data that the canonical climatological expectation is not met over the limited sampling period of a week. For example, the background POC decreased poleward in the open ocean (Transects 1 and 2; T1 and T2, respectively, hereafter) (Table 1, Figures 2, 3); while the background Chl-*a* increased poleward, the NF average decreased poleward, showing that there can be differences based on how the background conditions are estimated. The background SST, temperature averaged over the top 50 m, and other chemical (nitrate, phosphate, silicate, and PN) and biological (TBC, zooplankton and PP) variables, however, increased poleward (Table 1). Transect 3 (T3) was situated in the transition zone between the shelf and the open-ocean regime; the background conditions for this transect generally behaved as for T1 and T2, but the background nitrate, phosphate, POC, PP, and TBC decreased from T2 to T3 (Table 1).

Transects 4 and 5 (T4 and T5; see Figures 5, 6), which lie partly on the shelf, fall roughly in the same latitude band as T3, and were sampled shortly before it. The background SST and average temperature in the top 50 m (Chl-*a*) decreased (increased) inshore, from T4 to T5; a large shoreward increase, from T4 to T5, was seen in POC, PP; zooplankton, and TBC, while nutrients (nitrate, phosphate, silicate) and PN decreased inshore (Table 1). Nitrate and silicate concentrations increased from the open ocean towards the shelf (comparing values for T1 and T2 with those for T4 and T5 in Table 1). Comparing the mean of T1 and T2 with that of T4 and T5 shows that the mean phytoplankton biomass, zooplankton biomass, and total bacterial abundance also increased inshore. In general, therefore, there was significant spatial variation in the background conditions under which the fronts formed.

3.2. The conditions in the frontal zones

Fronts were sampled on each of the five transects and are described in Figures 2-6. Each of these figures presents the remote-sensing (panels on the left) and *in situ* (panels on the right) data for a transect. The SST snapshot on a few occasions is plotted in the upper left panels (the panels with a colour fill image) and the fronts that existed at that time are marked on them. As mentioned in Section 2.1, these snapshots are from different satellites. Each of the bottom left panels (the ones without the SST data) tracks a specific front over the duration of sampling; the colour used gives the time (listed at the bottom of the left panels) at which the front was mapped in the satellite SST data. As can be seen from these panels, the fronts tend to move over time and this movement is tracked using the colour coding: the black curve represents the start and the red curve the end of the front; the grey and pink curves represent the front before and after the sampling duration, respectively; the other colours represent the front at specific times during the sampling of the transect and the date and time of the satellite image are given below these panels. These panels summarize the movement of the front: the fronts are tracked, with the SST contoured in the background, in the supplementary material (Figures S2 to S7) to show how the front evolves from the time it forms to the time it is sampled. Each of these fronts is named to permit its association with the *in situ* data: for example, T1A refers to Front A in Transect 1 (mapped in the first of the two bottom-left panels of Figure 2); this front was first sampled around midnight on 25-26 January and is marked accordingly at the top of the right panels. Another front, T1B, also passed over this transect, but it moved away before the relevant stations were sampled (second of the two bottom-left panels of Figure 2). In view of the frontal activity impacting even the NF regime, we use the transect average (second definition) to represent the background for estimating the change within the fronts with respect to the background.

T1 was covered in just a day, starting around 1620 IST (UTC+0530) on 25 January until 1420 IST on 26 January. Front A in T1 (Front T1A) first appeared on 22 January and it moved northwestward, but with significant changes in shape over time (see the first of the two bottom-left panels in Figure 2). Hence, this front was sampled twice over the transect, late on the night of 25 January (station T1c) and in the early hours of 26 January (stations T1f and T1g), but with two intervening stations (T1d and T1e) that fall in the NF regime. The reason for this front being sampled a second time even though the transect was mapped monotonically from northwest to southeast is the remarkable change in the shape of the front from 2207 hours on 25 January (cyan curve) to 0207 hours on 26 January (light brown curve); this change can be seen more clearly in the supplementary material: Figure S2 shows the evolution of T1A. Depth-integrated nutrient concentration in the upper 50 m was higher

in the front compared to the background (3, 1 and 4% respectively for nitrate, phosphate and silicate respectively), but depth-integrated Chl-*a* was lower (5%) in the frontal regime (Table 1): the highest Chl-*a* was seen around 30 m at the southern end of the transect in the NF regime. Note that Front T1B passed through this station (T1j) just over a day (0916 hours on 25 January: see the orange curve in the bottom panel on the left of Figure 2) before it was sampled (afternoon of 26 January, top right panel), suggesting that the ecosystem in the NF regime is as dynamic, owing to advection (of fronts), as the frontal regime. A similar residual Chl-*a* signature was noted during the earlier cruise in the region of frontal activity even after the front had been advected away (Vipin et al., 2015) and it was evident in the HPLC-measured Chl-*a* too (Roy and Anil, 2015), implying that this residual signature is real. The Fv/Fm ratio was slightly higher in the frontal regime compared to the background, suggesting the presence of more active phytoplankton cells in the frontal regime. As a result, higher PP (11%), TBC (21%), and zooplankton biomass (40%) were observed in the frontal regime. Owing to enhanced biological activity in the frontal regime, higher POC (4%) and PN (7%) were observed, with their ratios close to the Redfield ratio (Table 1), suggesting that *in situ* production is likely to be the contributing factor.

The SST in T2 increases monotonically to the south (Figure 3). Note that this transect was not sampled in order along the track. T2A, is the third of the four stations in the contour plots in Figure 3. Front T2A first appeared on 22 January and it moved northwestward. During the period of interest, which was just over 12 hours from 2120 hours on 24 January to around 1000 hours on 25 January, Front T2A was confined mostly to the north of station T2a, but it passed through T2a when it first appeared on 22 January. Front T2B first moved southeastward and then northwestward (Figure S3): a change in the current direction is not apparent in the surface current in the OSCAR (Ocean Surface Current Analysis Real-Time) product (Bonjean and Lagerloef, 2002), but ADCP (acoustic Doppler current profiler) data from 20°N at 69.2°E (Amol et al., 2014) show a reversal in the current at 40 m for about four days during this period (Suchandan Bernal, personal communication, 2017), suggesting that the WICC may indeed have reversed during this period. The OSCAR current is estimated from satellite measurements and does not have the temporal resolution to capture such a short time scale. In the satellite data, Front T2B is confined to the southeast of station T2a, but it is seen close to this location on the morning of 24 January, about 12 hours before sampling. It is at this station, which appears to lie between Fronts T2A and T2B, that the Chl-*a* peak was observed in the upper 30 m (Figure 3). The temperature decrease in Front T2A compared to the background was the higher (0.91° C) compared to the other fronts (~0.2-0.46° C). As with T1A, there was a significant increase in the depth-integrated Chl-*a* (by 70%), nutrients (3-4%), Fv/Fm (2%),

TBC (15%), and zooplankton biomass (54%) at station T2B, where frontal activity was observed a few hours before it was sampled (see satellite maps in Figures 3 and S3). The increase in TBC was higher in T2B than in the other fronts sampled in this study.

Fronts T3A (Figure S4) and T3B (Figure S5) on T3 were observed on 30 January between 0100 and 1140 IST and relatively lower temperature and higher Chl-*a* were observed in T3A and T3B (Figure 4). T3 is situated between the shelf and open-ocean regimes and the front showed a higher concentration of nutrients (2-18%), Chl-*a* (13%), PP (8%), TBC (12%), and zooplankton biomass (1%) compared to the background (Table 1).

T4 and T5 were located in the shelf regime, where the biological response was significantly different from that in the open-ocean transects owing to a much higher zooplankton biomass on the shelf (Table 1). Higher Chl-*a* (4%) was observed in the fronts T4A (Figure S6) and T5A (Figure S7) and presence of subsurface Chl-*a* was observed in the NF regimes (Figures 5, 6). Fronts had passed through these stations before they were sampled. See, for example, the satellite data for Front T4B (Figure S6) in the bottom-left panel in Figure 5: Front T4B passes through stations T4g and T4h the same day, but several hours prior to sampling. So this pattern of frontal activity leading to subsurface Chl-*a* maxima is quite common for transects surveyed in this cruise as well as in the cruise described in Vipin et al. (2015). An increase in nutrients Chl-*a*, Fv/Fm, and zooplankton biomass was observed in the Fronts T4A and T5A compared to the background by 2 to 41%.

3.3. Variation of the biogeochemical variables in the frontal and non-frontal regimes

Over all, the biological response is not uniform in the open ocean and shelf regimes in the NEAS. An increase in Chl-*a* concentration and Fv/Fm compared to the background has been noted in the frontal regime in four of the five transects; the increase in phytoplankton cell activity, inferred from Fv/Fm, suggests an injection of nutrients into the ML in the frontal regimes. In spite of an increase in the nutrients in all frontal regimes sampled, the magnitude of increase in the phytoplankton biomass was not uniform in all the fronts (Figures 2-6; Tables 1, 3). For instance, the depth-integrated phytoplankton biomass (as Chl-*a*) was higher at Fronts T2A, T3A, T4A, and T5A (4-70%) compared to the background for these transects, but it was lower by 5% in Front T1AB (hereafter, AB represents an average over fronts A and B; see Table 1, which lists the properties for these averages). The phytoplankton biomass increased in all shelf fronts (4-13%), but decreased in one open-ocean front (by 5% in T1) and increased in other open-ocean front (70% in T2). Primary production increased by 7-90% in Fronts T1A, T3AB (T3AB implies an average for T3A and T3B), and T4A, but decreased by 4-15% in Fronts T2A and T5A compared to the respective background conditions

(Table 3). Though the percentage increase in biomass in the fronts compared to the background was similar in the open-ocean (39-54%) and shelf (12-41%) fronts, the much higher background zooplankton biomass (by more than three times) on the shelf compared to the open ocean implies a significantly higher increase in absolute abundance on the shelf (Table 1). In contrast, the open-ocean fronts showed a higher increase of TBC (21-116%) compared to the shelf fronts, where an increase of 33% in T4 was matched by a similar decrease in T5. The data therefore suggest the possibility that bacteria respond more in the open-ocean fronts, while zooplankton responds in the shelf front. If this inference, admittedly based on a small sample size, is borne out by more data, it would imply that the microbial loop dominates in the open ocean and the classical food web on the shelf.

4. Discussion

4.1. Variable biological response in the shelf and open-ocean fronts

The data from the five transects suggest that fronts tend to be more productive than their surroundings owing to injection of nutrients into the ML. The Fv/Fm ratio was higher in the frontal regime compared to the background in four of the five transects, with there being no difference in the ratio for T3 (Table 1), suggesting that phytoplankton cells were relatively healthy within the fronts than in the NF regimes.

4.1.1. Influence of background or initial conditions

The response of different biological elements of the ecosystem is not uniform in all the fronts sampled. For instance, increase in TBC was noticed in the open-ocean fronts, while enhanced zooplankton abundance was observed in the shelf fronts. Enhanced response of zooplankton in the shelf fronts may be boosted by higher background (initial conditions) values: for instance, the background zooplankton biomass was higher on the shelf (813-1520 mg m⁻²) compared to the open ocean (324-479 mg m⁻²; Table 1); this difference between the response in the open-ocean and shelf fronts is summarized in Fig. 8. This potential influence of the background conditions, which represent the initial conditions when we consider the temporal evolution, on the conditions that prevail in a front that forms in the region suggests that the background conditions must be factored into any inferences drawn regarding the evolution of the ecosystem within such fronts.

What complicates the determination of the background or initial conditions for a front is that it is dynamic, i.e., a front is advected by the mean current and is also likely to be affected by the mesoscale eddy field. Hence, the initial conditions can be split into three parts. The first part of the

initial condition is provided by the slowly evolving seasonal cycle, whose spatial scale is also large. The second and third parts of the initial condition are due to intraseasonal variability, but this period range from a few days to ~90 days has to be split further into two parts. One part may be considered independent of fronts and therefore has a time scale greater than that associated with the fronts. In other words, this part of the background state has a time scale of the order of 15-90 days because the life span of a typical front is of the order of 1-2 weeks (as discussed in Section 3). Time scales shorter than ~15 days may be affected by frontal activity. As seen in transects 1-4, fronts were seen at different locations on the transects through the sampling period. Since the physical front moves and takes with it the nutrient-injecting mechanism and all else that is subject to advection, including phytoplankton and zooplankton, a front constitutes a Lagrangian system. Hence, a front can modulate its surroundings and therefore the background conditions. It is difficult, therefore, to distinguish a frontal regime from the non-frontal regime, which essentially is the surrounding waters, from the perspective of ecosystem evolution when sampling along a section across the front. The physical signature of the front seems to move with it, but a residual signature can be left behind: Vipin et al. (2015) noted that the residual Chl-*a* signature in the regime of frontal activity was not associated with a physical signature. Temperature fronts form periodically in the northern Arabian Sea during winter at variable time scales (hours to days) and the seasonally integrated data of frontal locations show that fronts traversed across the northern Arabian Sea during the winter monsoon (Fig. S8). Since nutrients are injected into the ML in a frontal regime and there is a biological response to this increased availability of nutrients, the air-sea exchange of gases may differ from the background in such frontal regimes. For example, analysis of data from these transects and two others farther south suggest that the pCO₂ levels were higher in the frontal regimes compared to the NF regimes (Sarma et al., 2015).

While direct current measurements at the surface are not available for this region and one has to rely on satellite-based current estimates, data from moorings equipped with acoustic doppler current profilers (ADCPs) show that the alongshore current at ~50 m on the continental slope at ~20°N exceeds 20 cm s⁻¹ roughly 15% of the time (see Figure 3a in Amol et al., 2014). The WICC is the strongest during the winter monsoon (Figures 2a and 9 in Amol et al., 2014), when its magnitude can exceed 40 cm s⁻¹. A speed of 20 (40) cm s⁻¹ translates to a distance of ~17 (34) km in a day; this distance exceeds the typical width of ~10 km associated with these fronts, making advection an important factor in the evolution of fronts and frontal ecosystem in the NEAS.

4.1.2. *Impact of age of the front*

Jones and Halpern (1981) suggested that response of biology may show a lag of several days from the formation of the front. Hence, the age of the front may have a significant impact on the response of various components of the ecosystem to the nutrients injected in a frontal system and the role of persistence of fronts is noted by Solanki et al. (2003, 2010) in their study of PFZs. In the NEAS, an increase in TBC was noticed in Fronts T1A and T2A (open-ocean fronts), but the response was significantly lower in the former (72%) than in the latter (249%). The stronger response in Front T2A may be related to it being older (~6 days) compared to Front T1A (~3.3 days; Table 2). Likewise, though an increase in zooplankton biomass was noticed in all the shelf fronts, the response was higher in the older Front T4A (~149%, 9-11 days old) compared to the younger Front T5A (23%; 0.5 days). Though the data are limited, this relation of the biological response to the age of the front suggests that the age is important for determining the biological response in a frontal regime, irrespective of the background (shelf or open ocean) or initial conditions.

Phytoplankton primary production (PP) did not show any relation with age of the front. For instance, higher PP was noticed in Front T1A, which was ~3.3 days old; the background zooplankton biomass was the lowest in T1, suggesting that lower grazing might have facilitated enhanced PP, but this relation does not hold for all fronts and the ecosystem response is complex.

4.1.3. *Mixing and advection*

The horizontal scale, or width of the fronts, is of the order of 10 km (Vipin et al., 2015). The length scale over which the wind speed changes, however, is larger (Shankar et al., 2015), ruling out classical wind-driven or convective mixing as the cause of the lower temperature and enhanced nutrients in the fronts. The horizontal length scales associated with these fronts is too small to show up in satellite altimeter data, which have a spatial resolution of roughly 25-35 km (AVISO, 1996).

It is possible, nevertheless, to speculate on the possible causes of the lower temperature in the fronts. As seen in Fig. 1, which presents the average SST for the sampling period of a week, the SST shows a maximum in the neighbourhood of the continental slope (see the shelf break in Fig. 1) towards the south of the NEAS. It decreases poleward and offshore and inshore of the peak around the shelf break. The poleward decrease is expected from climatology (Chatterjee et al., 2012), and so is the decrease in SST to the west of the poleward WICC (Shankar et al., 2015). The SST decreases on the inner shelf as well. A careful examination of the satellite data and fronts in Figures S2-S7 shows that these fronts occur at the northern, western, and eastern “edges” of this patch of warm surface water

advected poleward by the WICC. The shape of the fronts and their deformation in time suggests horizontal mixing, which we speculate is driven by barotropic instability. Barotropic instability has been shown to play a significant role in the northern and western Bay of Bengal in the regime of the East India Coastal Current (Mukherjee et al., 2017; Mukherjee, 2017), and the patterns seen in the satellite SST data suggest that this instability may be important for frontal activity in the NEAS. The currents associated with this instability would advect water along the front, making possible a transfer of water — and all properties — across the shelf break when the front extends across the shelf-slope divide. In such cases, one can expect the shelf waters, which tend to be more productive, to influence the slope fronts.

The model simulations for the Bay of Bengal also suggest significant baroclinic instability as well (Mukherjee et al., 2017; Mukherjee, 2017), and we speculate that it will play a significant role in the NEAS as well. We speculate that instabilities may constitute an important mechanism for injecting nutrients from below into the ML in the frontal regimes. Model studies with high-resolution general circulation models are required to test this speculation.

4.2. *Frontal zones and potential fishing zones (PFZ)*

The motivation for this study of SST fronts lies in their implication for fisheries as satellite SST and Chl-*a* data are used to identify PFZs (Solanki et al., 2001, 2003, 2010). The empirical model used for identifying PFZs led to an advisory being issued for Fronts T3A and T4A (Figs. 4,5) during our sampling (Fig. 1); these are the oldest of the fronts surveyed (Table 2, Fig. 9). No advisory was issued for the other fronts, the oldest of which was T2A (~6 days, Table 2). Although we were not geared up with fishing tools on board our vessel, we did find higher fishing activity by over 200 boats (count based on ship's radar system) near Front T4A (see Fig._S9) and about 100 boats were noticed in the regime of Front T3A. Since the frontal age is not explicitly factored into the advisory model, this link between the PFZs and the older fronts occurs through the satellite Chl-*a* data, with the satellite Chl-*a* tending to be higher for these fronts.

Curiously, in situ measurements show that the highest increase in surface Chl-*a* compared to the NF regime occurred in Front T2A ($1.1 \pm 0.5 \text{ mg m}^{-3}$ versus $0.5 \pm 0.3 \text{ mg m}^{-3}$), and the difference was insignificant in the other fronts (Sarma et al. 2015). In contrast, it is the depth-integrated Chl-*a* (Table 1) that was higher in the frontal regime compared to the background conditions, with Front T1A being the only exception. This difference between the surface and depth-integrated Chl-*a* signatures in the frontal regime suggests that the depth-integrated Chl-*a* may be a better marker of PFZs than the surface Chl-*a*. It has been shown in the Atlantic and Pacific Oceans that the depth-

integrated Chl-*a* can be obtained from surface Chl-*a* (Frolov et al. 2012); an effort is required to develop similar relations for the Indian seas.

This study suggests that factors other than SST and Chl-*a*, as measured by a satellite, impact the biological response in frontal systems. The background or initial conditions — whether the front occurs on the shelf or in the open ocean, the average productivity in the NF regime, which constitutes the surroundings in which a front exists, the MLD, and the history of frontal activity in the region — can lead to significantly different ecosystem evolution pathways. All these variables, and so also the age of the front, which can be determined from the SST data, can help improve the PFZ advisory model. High-resolution numerical models do show barotropic and baroclinic instability and it is useful to use hindcasts to see if these instabilities play a role in the evolution of these SST fronts.

The fronts identified as PFZs (T3A and T4A) also exhibited a higher zooplankton biomass with respect to the background conditions (Table 1). Zooplankton constitute a more direct food for the fish and are therefore more likely to be a significant element of PFZs, but they are not as easy to measure without in situ sampling as SST or Chl-*a* or the other variables discussed above.

The sample size in this paper is admittedly small for drawing robust conclusions, but the data nevertheless point to the potential for improving PFZ advisories.

5. Summary and directions for the future

We have described the result of sampling along five transects that cut across SST fronts in the NEAS during January-February (winter monsoon) 2014. The data suggest that temperature fronts even in the tropical regime of the Indian EEZ are active biological hotspots owing to significant injection of nutrients into the ML. Analysis shows that the biological response to this availability of nutrients, however, depends on several factors.

The background and initial conditions matter for the evolution of a front. The response seems to be different in fronts located on the shelf and in the open ocean (Fig. 9). In the shelf fronts, the classical food web seems to be operational, with a significant increase in the zooplankton biomass; in the open-ocean fronts, in contrast, the microbial loop seems to dominate, with a significant increase in TBC (Table 1). Since the background zooplankton biomass was higher on the shelf, it is not only the initial physical conditions that vary from the shelf to the open ocean, but also the biological initial conditions, and these differences are important for the evolution of a front. The conditions in which a front forms and evolves can vary in time as well because there is a well-defined seasonal cycle on

which intraseasonal variability is superimposed. Our data show, however, that the advection of fronts adds to this intraseasonal variability in the background conditions. In other words, since a front is not stationary, it influences its “surroundings” and modulates the background conditions in which subsequent fronts form and evolve. This modulation of the background conditions due to advection of fronts can therefore influence the average concentration of nutrients or of biomass. While the influence of advection on biology is known in stronger fronts seen at higher latitudes, there is a dearth of literature on the kind of short-lived, short-scale tropical fronts described in this study.

Since the biology takes time to respond to the physico-chemical forcing in the form of increase in nutrients, the age of the front, or its persistence (Solanki et al., 2003, 2010), matters. Higher biological response was noted in the older fronts T3A and T4A (see Table 1). The age is likely to be even more important for the open-ocean fronts because the microbial loop seems to be dominant in these fronts. Since this lag depends on the trophic level and varies across species within each trophic level, the ecosystem response to the availability of nutrients in a frontal system is complex.

The data also suggest that depth-integrated concentrations capture the biological response in a frontal system better than do surface values: the depth-integrated Chl-*a* (Table 1) behaved differently from the surface Chl-*a* (Sarma et al. 2015). It may be important to develop algorithms to estimate depth-integrated Chl-*a* from satellite Chl-*a* measurements for the Indian seas, as has been done for the Atlantic and Pacific Oceans (Frolov et al. 2012). This difference between surface and depth-integrated values may explain why the higher fish catch in PFZs in the NEAS was 80% higher in the 50-100 m depth regime compared to the NF regime, while the increase in the PFZs was 68% in the 30-50 m depth regime (Solanki et al. 2001, 2003). The fish caught in this region were mainly carnivorous, such as Pomfret (*Pampus argentus*), Ribbon fish (*Trichiurus sp*), catfish (*Trachysurus caelatus*), and Bombay duck (*Harpadon nehereus*), and the fishing was carried out using mechanized multi-day trawlers, mechanized *dol* netters, and outboard gill netters. Since these fish do not directly depend on phytoplankton but some of them feed on larger zooplankton, the lag period for this fish to respond to increase in primary and secondary producers must be longer, again pointing to the implication of the age of the front for PFZs. Equally important is the role of advection, which makes it difficult to issue an advisory. Earlier, the PFZ advisories were deemed valid for three days (Nammalwar et al., 2013; Subramanian et al., 2014; George et al., 2014), over which the data suggest that a front can be advected over a hundred km, an order of magnitude greater than the typical frontal width of ~10 km. Of late, however, INCOIS has curtailed the validity of the advisories to 24 hours,

but current data (Amol et al., 2014) suggest that significant advection is possible even over this duration. PFZ advisories need to factor in the potential advection for greater accuracy.

Therefore, the SST fronts seem to constitute a necessary condition for the existence of PFZs, but they are not sufficient. Other factors like the background or initial conditions and the age of the front influence the biological response. Including these additional factors can help improve PFZ advisories. For converting the advisories into forecasts, it will be necessary to generate the statistics of generation of fronts in the high-resolution general circulation models used for forecasting and improve the ability of these models to simulate the observed distribution and evolution of fronts.

Some of the questions raised in this paper can be answered by conducting mesocosm and Lagrangian experiments. Mesocosm experiments are required to ascertain the biological response to nutrient enrichment under a variety of conditions. Lagrangian experiments are required to track the evolution of a front as it is advected across the region of study. In contrast, time-series measurements may capture instances of frontal activity at a location; such observations can complement the Lagrangian experiments in which a front is identified and tracked over time.

That the temperature fronts are biologically active sites makes them important not only for the ecosystem evolution and fisheries, but also for climate. The increased biological activity in a front must lead to a different budget vis-a-vis the NF regime, implying that the fronts may play an important role in the carbon and nitrogen cycles. For example, heterotrophy is dominant at the surface, as seen in the undersaturation of dissolved oxygen and supersaturation of $p\text{CO}_2$: enhanced $p\text{CO}_2$ levels (by 3 to 50 μatm) have been measured within the fronts in the NEAS, suggesting that temperature fronts may be a potential source for atmospheric CO_2 (Sarma et al., 2015). On the other hand, a part of the organic matter produced within the front will be transported to the deep ocean, potentially impacting the intensity of OMZ and denitrification and leading to patchiness in the chemical data as obtained from cruises. Therefore, it is necessary to evaluate the impact of temperature fronts on sinking organic carbon fluxes, intensification of the OMZ, and meso- and bathypelagic ecosystems.

Acknowledgements

We acknowledge Mr. K. Sarkar and Mr. P. Vipin for processing the remote-sensing data that were transmitted to the research vessel to guide us to the frontal locations. Dr. S.S.C. Shenoi and Mr. E. P. Rama Rao of INCOIS, Hyderabad are acknowledged for their support to supplying near-real time satellite SST data for identifying fronts in the study region. Mr. Amol Kambli, Mr. Rahul Khedekar,

Mr. P. Vipin, and Ms. R. Remya helped with the figures. The service rendered by CSIR-NIO's ship cell personnel for CTD operations is highly appreciated. The master of the ship and other crew members are thanked for their support during the cruise. Ocean Data View (ODV) and Ferret were used for analysis and graphics and STATISTICA was used for statistical analysis. This paper has benefited significantly from comments from two anonymous reviewers and the handling editor: we acknowledge this contribution. This is CSIR-NIO contribution XXXX.

References

- Amol, P., Shankar, D., Fernando, V., Mukherjee, A., Aparna, S.G., Fernandes, R., Michael, G.S., Khalap, S.T., Satelkar, N.P., Agarvedekar, Y., Gaonkar, M.G., Tari, A.P., Kankonkar, A., Vernekar, S.P. 2014. Observed intraseasonal and seasonal variability of the West India Coastal Current on the continental slope. *J Earth Syst Sci* 123:1045–1074
- AVISO (1996) AVISO User Handbook: Merged TOPEX/Poseidon Products; Technical report; Toulouse, France.
- Banse, K. 1968. Hydrography of the Arabian Sea shelf of India and Pakistan and effects on demersal fishes. *Deep Sea Res* 15:45–79
- Barber, R. T., J. Marra, R. C. Bidigare, L. A. Codispoti, D. Halpern, Z. Johnson, M. Latasa, R. Goericke, and S. L. Smith (2001), Primary productivity and its regulation in the Arabian Sea during 1995, *Deep Sea Res., Part II*, 48, 1127–1172
- Basterretxea, G, Aristegui, J., 2000. Mesoscale variability in phytoplankton biomass distribution and photosynthetic parameters in the Canary-NW African coastal transition zone. *Mar. Ecol. Prog. Ser.* 197, 27-40.
- Behrenfeld, M.J., Falkowski, P.G., 1997. Photosynthetic rates derived from satellite-based chlorophyll concentration. *Limnol. Oceanogr.* 42, 1-20.
- Bonjean, F., Lagerloef, G.S.E., 2002. Diagnostic model and analysis of the surface currents in the Tropical Pacific Ocean. *J. Phys. Oceanogr.* 32, 2938–2954.
- Belkin, I., Cornillon, P.C., and Sherman, K. 2009. Fronts in Large Marine Ecosystems, *Progr. Oceanogr.*, 81, 223-236.
- Benoit-Bird, K.J., 2009. Dynamic three-dimensional structure of zooplankton thin layers is affected by foraging fish. *Mar. Ecol. Prog. Ser.* 393, 61-76.
- Bhattathiri, P.M.A., Pant, A., Sawant, S., Gauns, M., Matondkar, S.G.P., Mohanraju, R., 1996. Phytoplankton production and chlorophyll distribution in the eastern and central Arabian sea in 1994-1995. *Curr. Sci.* 71, 857-862.
- Bjorkstedt, E.P., Rosenfeld, L.K., Grantham, B.A., Shkedy, Y., Roughgarden, J., 2002. Distributions of larval rockfishes *Sebastes* spp. Across nearshore fronts in a coastal upwelling region. *Mar. Ecol. Prog. Ser.* 242, 215-228.

- Borges, A.V., and Frankignoulle, M., 2003. Distribution of surface carbon dioxide and air-sea exchange in the English Channel and adjacent areas. *J. Geophys. Res.* 108, <http://dx.doi.org/10.1029/JC000571>.
- Boutin, J., Merlivat, I., Henocq, C., Martin, N., Sallee, J.B., 2008. Air-sea CO₂ flux variability in frontal regions of the Southern Ocean from carbon interface ocean atmosphere drifters. *Limnol. Oceanogr.* 53, 2062-2079.
- Brink, K.H., 1987. Upwelling fronts: implications and unknowns. In: *The Benguela and Comparable Ecosystems*. (A.I.L. Payne, J.A. Gulland, and K.H. Brink, Eds.) *S. Afr. J. Mar. Sci.*, 5, 3-9.
- Brown, S.L., Landry, M.R., Selph, K.E., et al. 2008. Diatoms in the desert: phytoplankton community response to a mesoscale eddy in the subtropical North Pacific. *Deep-Sea Res.*, II 55, 1321-1333.
- Brodeur, R.D., Wilson, M.T., Napp, J.M., Stabeno, P.J., Salo, S.A., 1997. Distribution of juvenile Pollock relative to frontal structure near the Pribilof Islands, Bering Sea. In: *Forage fishes in marine ecosystems. Proceedings of the International Symposium on the role of Forage Fishes in Marine Ecosystems*. University of Alaska Sea Grant, AK-SG-97-01, Fairbanks, pp. 573-589.
- Carritt, D.E., and Carpenter, J.H., 1966. Comparison and evaluation of currently employed modifications of Winkler method for determining dissolved oxygen in seawater a Nasco report. *J. Mar. Res.* 24, 286.
- Cayula, J.-F., Cornillon, P., 1992. Edge detection algorithm for SST images. *Journal of Atmospheric and Oceanic Technology* 9 (1), 67–80
- Chatterjee, A., Shankar, D., Shenoi, S.S.C., Reddy, G.V., Michael, G.S., Ravichandran, M., Gopalkrishna, V.V., Rao, E.P.R., Bhaskar, T.V.S.U., Sanjeevan, V.N. 2012. A new atlas of temperature and salinity for the North Indian Ocean. *J Earth Syst Sci* 121:559–593.
- Chen, J.C., 1983. Interpretation of the temperature distribution in winter of the northern part of the south China Sea. *Acta Oceanol. Sin.* 5, 391-395.
- Clayton, S., Nagai, T., Follows, M.J., 2014. Fine scale phytoplankton community structure across the Kuroshio Front. *J. Plank. Res.* 1-14, doi: 10.1093/plankt/fbu020.
- Coyle, K.O. and Cooney, R.T., 1993. Water column sound scattering and hydrography around the Pribilof Islands. *Cont. Shelf Res.* 13, 803-827.
- Decker, M.B., and Hunt Jr., G.L., 1996. Foraging by murre (Uria spp.) at tidal fronts surrounding the Pribilof Islands, Alaska, USA. *Mar. Ecol. Prog. Ser.* 139, 1-10.
- Dengler, A.T., 1985. Relationship between physical and biological processes at an upwelling front off Peru, 15°S. *Deep-Sea Res.* 32, 1301-1315.
- De Sousa, S.N., Kumar, M.D., Sardesai, S., Sarma, V.V.S.S., and Shirodkar, P.V., 1996. Seasonal Variability in oxygen and nutrients in the central and eastern Arabian Sea, *Curr. Sci.* 71, 847-851.
- Dugdale, R.C., and Wilkerson, F.P., 1986. The use of ¹⁵N to measure nitrogen uptake in eutrophic oceans: experimental considerations. *Limnol. Oceanogr.* 31, 673-689.

- Fiala, M., Sournia, A., Claustre, H., Marty, J.C., Prieur, I., Vétion, G., 1994. Gradients of phytoplankton abundance, composition and photosynthetic pigments across the Almeria-oran front (SW Mediterranean Sea). *J. Mar. Syst.* 5, 223-233.
- Flint, M.V., Sukhanova, I.N., Kopylov, A.I., Poyarkov, S.G., and Whitley, T. E., 2002. Plankton distribution associated with frontal zones in the vicinity of the Pribilof Islands. *Deep-Sea Research II* 49, 6069-6093.
- Franks, P.J.S., 1992. Phytoplankton blooms at fronts: Patterns, scales, and physical forcing mechanisms, *Reviews Aquat. Sci.* 6, 121-137.
- Frolov, S., Ryan, J.P., and Chavez, F.P., 2012. Predicting euphotic-depth-integrated chlorophyll-a from discrete-depth and satellite-observable chlorophyll-a off central California, *J. Geophys. Res.* 117, doi: 10.1029/2011JC007322.
- Garcia, H.E., Locarnini, R.A., Boyer, T.P., Antonov, J.I., Baranova, O.K., Zweng, M.M., Reagan, J. R., and Johnson, D.R., 2014. World Ocean Atlas 2013, Vol. 4, Dissolved Inorganic Nutrients (Phosphate, Nitrate, Silicate), NOAA Atlas NESDIS 76, edited by A. Mishonov, 25 pp., U.S. Gov. Print. Off., Washington, D. C.
- Genin A., 2004 Biophysical coupling in the formation of zooplankton and fish aggregations over abrupt topographies. *J. Mar. Sys.* 50, 3-20.
- Genin, A. Jaffe, J.S., Reef, R., Richter, C., and Franks, P.J.S., 2005. Swimming against the flow: a mechanism of zooplankton aggregation. *Science* 308, 860-862.
- George, G., Sarma, K., Bharathi, G., Kaliyamoorthy, M., Krishnan, P., and Kirubasankar, R., 2014. Efficacy of different modes in disseminating Potential Fishing Zone (PFZ) forecasts – a case study from the Andaman and Nicobar Islands, *Indian J. Fish.* 61, 84-87.
- Grashoff, K., Ehrhardt, M. and Kremling, K. (eds.) 1992. *Methods of Seawater Analysis*. Verlag Chemie, New York, NY, 419 pp.
- Hama, T., Miyazaki, T., Ogawa, Y., Iwakuma, T., Takahashi, M., Otsuki, A., Ichimura, S., 1983. Measurement of photosynthetic production of a marine phytoplankton population using a stable ¹³C isotope. *Mar. Biol.* 73, 31-36.
- Holligan, P.M., Williams, P.L., Purdee, D., Harris, R., 1984. Photosynthesis, respiration and nitrogen supply of plankton populations in stratified, frontal and tidally mixed shelf waters. *Mar. Ecol. Prog. Ser.* 17, 201-213.
- Jacquet, S., Prieur, L., Avois-jacquet, C., et al. 2002. Short-timescale variability of picoplankton abundance and cellular parameters in surface waters of the Alboran Sea (Western Mediterranean). *J. Plankton. Res.* 24, 635-651.
- Jones, B.H., Halpern, D., 1981. Biological and physical aspects of a coastal upwelling event observed during March-April 1974 off northwest Africa. *Deep-Sea Res.* 28, 71-81.
- Jordon, M.B., Joint, I.R., 1984. Studies on phytoplankton distribution and primary production in the western English Channel in 1980 and 1981. *Cont. Shelf. Res.* 3, 25-34.

- Klein, P., Lapeyre, G., 2009. The oceanic vertical pump induced by mesoscale and submesoscale turbulence. *Ann. Rev. Mar. Sci.* 1, 351–375.
- Landaeta, M.F., Castro, L.R., 2006. Larval distribution and growth of the rockfish *Sebastes capensis* (Sebastidae, Pisces) in the fjords of Southern Chile, *ICES J. Mar. Sci.* 63, 714-724.
- Lévy, M., Klein, P., Treguier, A., 2001. Impact of sub-mesoscale physics on production and subduction of phytoplankton in an oligotrophic regime. *J. Mar. Res.* 59, 535-565.
- Lévy, M., Andre, J.-M., Shankar, D., Durand, F., Shenoi, S.S.C., 2006. A quantitative method for describing the seasonal cycles of surface chlorophyll in the Indian Ocean. In: Frouin, R.J., Agarwal, V.K., Kawamura H., Nayak S., Pan D. (eds) *Remote sensing of the marine environment, Proceedings of SPIE*, vol 6406.
- Li, L., Guo, X.G., Wu, R.S., 2000. Oceanic fronts in southern Taiwan strait. *J. Oceanogr.* 19, 147-156.
- Lu, G.M., Wang, H., Sun, S., et al. 2003. Numerical study on the velocity structure around tidal fronts in the Yellow Sea. *Adv. Atmos. Sci.* 20, 453-460.
- Lu, X.G., Qiao, F.I., Xia, C.S., et al. 2010. Upwelling and surface cold patches in the Yellow Sea in summer: effects of tidal mixing on the vertical circulation. *Cont. Shelf. Res.* 30, 620-632.
- Madhupratap, M., Prasannakumar, S., Bhattathiri, P.M.A., Raghukumar, S., Nair, K.K.C., Ramaiah, N. 1996. Mechanism of biological response to winter cooling in the northeastern Arabian Sea. *Nature* 384, 549–552
- Mahadevan, A., Thomas, L., and Tandon, A., 2008. Comment on “Eddy/wind interactions stimulate extraordinary mid-ocean plankton blooms”, *Science*, 320, 448.
- Mavor, T.P., Bisagni, J.J., 2001. Seasonal variability of sea surface temperature fronts on Georges Bank. *Deep Sea Res.*, II, 48, 215-243.
- McCarthy, J.J., Garside, C., Nevins, J.L., Barber, R.T., 1996. New production along 140°W in the equatorial Pacific during and following the 1992 El Niño event. *Deep-Sea Research II* 43, 1065-1093.
- McCreary, J.P., Kundu, P.K., Molinari, R.L., 1993. A numerical investigation of dynamics, thermodynamics and mixed-layer processes in the Indian Ocean. *Prog. Oceanogr.* 31, 181–244.
- McGillicuddy, D. et al. 2007. Eddy/wind interactions stimulate extraordinary mid-ocean plankton blooms, *Science* 316, 1021-1026.
- McManus, M.A., Woodson, C.B., 2012. Plankton distribution and ocean dispersal. *J. Expt. Biol.* 215, 1008-1016.
- Miller, A.J., McWilliams, J.C., Schneider, N., Allen, J.S., Barth, J.A., Beardsley, R.C., Chavez, E.P., Chereskin, T.K., Edwards, C.A., Haney, R.L., Kelly, K.A., Kindle, J.C., Ly, L.N., Moisan, J.R., Noble, M.A., Niiler, P.P., Oey, L.Y., Schwing, F.B., Shearman, R.K., Swenson, M.S., 1999. Observing and modeling the California Current System. *EOSTrans. AGU* 80, 533–539.

- Mukherjee, A., Shankar, D., Chatterjee, A., and Vinayachandran, P.N., 2017. Numerical simulation of the observed near-surface East India Coastal Current on the continental slope, *Climate Dynamics*, doi:10.1007/s00382-017-3856-x, 2017.
- Mukherjee, A. 2017 Intraseasonal variability of currents along east coast of India, PhD thesis, Goa University, India.
- Munk, P., Hansen, B.W., Nielsen, T.G., Thomsen, H.A., 2003. Changes in plankton and fish larvae communities across hydrographic fronts off West Greenland. *J. Plankton Res.* 25, 815-830.
- Nagai, T., Tandon, A., Yamazaki, H., et al. 2012. Direct observations of microscale turbulence and thermohaline structure in the Kuroshio front. *J. Geophys. Res.* 117, C08013.
- Nammalwar, P.S., Satheesh, S., and Ramesh, R., 2013. Applications of Remote Sensing in the validations of Potential Fishing Zones (PFZ) along the coast of North Tamil Nadu, India. *Indian J. Geo-Mar. Sci.* 42, 283-292.
- Obenour, K.M., 2014. Temporal Trends in Global Sea Surface Temperature Fronts. Open Access Master's Theses.
- Owen, R.W. 1981. Fronts and eddies in the sea: mechanisms, interactions and biological effects. In: *The analysis of marine ecosystems* (ed. A.R. Longhurst), 233 pp, London, Academic Press.
- Petrusevics, P., Bye, J., Luick, J., Teixeira, C.E.P., 2011. Summer sea surface temperature fronts and elevated chlorophyll-a in the entrance to spencer Gulf, South Australia, *Cont. Shelf. Res.*, 41, 849-856.
- Pingree, R.D., Maddock, L., 1979. Tidal flow around an island with a regularly sloping bottom topography. *J. Mar. Biol. Assoc. U.K.* 59, 699-710.
- Pitcher, G.C., Boyd, A.J., Horstman, D.A., et al., 1998. Subsurface dinoflagellate populations, frontal blooms and the formation of red tide in the southern Benguela upwelling system. *Mar. Ecol. Prog. Ser.* 172, 253-264.
- Pollard, R.T., Regier, L.A., 1990. Large variations in potential vorticity at small scales in the upper ocean. *Nature*, 348, 227-229.
- Polovina, J.J., Howell, E., Kobayashi, D.R., and Seki, M.P., 2001. The transition zone chlorophyll front a dynamic global feature defining migration and forage habitat for marine resources. *Prog. Oceanogr.* 49, 469-483.
- Polovina, J.J., Howell, E.A., Kobayashi, D.R., and Seki, M.P. 2015. The transition zone chlorophyll front updated: advances from a decade of research. *Prog. Oceanogr.*, DOI: 10.1016/j.pocean.2015.01.006.
- Roy, R., Rajath, C., Vinayak, K., Krishna, M.S., Sarma, V.V.S.S., Anil, A.C., 2015. CHEMTAX-derived phytoplankton community structure associated with temperature fronts in the northeastern Arabian Sea. *J. Mar. Syst.* 144, 81-91.
- Resplandy, L., Boutin, J., Merlivat, I., 2014. Observed small spatial scale and seasonal variability of the CO₂ system in the Southern Ocean. *Biogeosciences*, 11, 75-90.

- Roy, R., Anil, A.C. 2015. Complex interplay of physical forcing and Prochlorococcus population in ocean. *Oceanography*, doi: 10.1016/j.pocean.2015.06.010.
- Rudnick, D.L., Luyten, J.R., 1996. Intensive survey of the Azores front: 1. Tracers and dynamics. *J. Geophys. Res.*, 101, 923-939.
- Sarma, V.V.S.S., Delabehera, H.B., Sudharani, P., Remya, R., Patil, J.S., Dessai, D., 2015. Variations in the inorganic carbon components in the thermal fronts during winter in the northeastern Arabian Sea, *Mar. Chem.* 169, 16-22.
- Sarma, V.V.S.S., M.S. Krishna, V.R. Prasad, B.S.K. Kumar, S.A. Naidu, G.D. Rao, R. Viswanadham, T. Sridevi, P.P. Kumar, N.P.C. Reddy, 2014. Distribution and sources of particulate organic matter in the Indian monsoonal estuaries during monsoon, *Journal of Geophysical Research (Biogeosciences)*, 11/2014,119, doi: 10.1002/2014JG002721.
- Schneider, D.C., Harrison, N.M., Hunt Jr. G.L., 1990. Seabird diet at a front near the Pribilof Islands, Alaska. *Studies in Avian Biology*, 14, 61-66.
- Schneider, N., Qiu, B., 2015. The atmospheric response to weak sea surface temperature fronts. *J. Atm. Sci.*, 72, doi: 10.1175/JAS-D-14-0212.1.
- Shankar, D., Remya, R., Vinayachandran, P.N., Charterjee, A., and Behera, A. 2016. Inhibition of mixed-layer deepening during winter in the northeastern Arabian Sea by the West India Coastal Current. *Climate Dynamics*, 47, 1049-1072.
- Shankar, D., Shetye, S.R. 1997. On the dynamics of the Lakshadweep high and low in the southeastern Arabian Sea. *J. Geophys. Res.*, 102, 12,551–12,562
- Shetye, S.R., Gouveia, A.D., Shenoi, S.S.C., Michael, G.S., Sundar, D., Almeida, A.M., Santanam, K. 1991. The coastal current off western India during the northeast monsoon. *Deep-Sea Res.* 38:1517–1529
- Solanki, H.U., Dwivedi, R.M., Nayak, S.R., 2000. Generation of composite image using OCM chlorophyll and NOAA AVHRR SST for locating potential fishing grounds. *Proceedings PORSEC 2000 Part II*, pp. 669-672.
- Solanki, H.U., Dwivedi, R.M., Nayak, S.R., Jadeja, J.V., Thakar, D.B., Dave, H.B., Patel, M.I., 2001. Application of Ocean Colour Monitor chlorophyll and AVHRR SST for fishery forecast: Preliminary validation results off Gujarat coast, northwest coast of India. *Indian Journal of Marine Sciences* 30, 132-138.
- Solanki, H.U., Dwivedi, R.M., Nayak, S.R., Somvanshi, V.M., Gulati, D.K., and Pattnayak, S.K., 2003. Fishery forecast using OCM chlorophyll concentration and AVHRR SST: validation results off Gujarat coast, India. *International Journal of Remote sensing*, 24, 3691-3699.
- Solanki, H.U., Prakash, P., Dwivedi, R.M., Nayak, S.R., Kulkarni, A., Somvamshi, V.S., 2010. Synergistic application of oceanographic variables from multi-satellite sensors for forecasting potential fishing zones: methodology and validation results. *International Journal of Remote sensing* 31, 775-789, doi:10.1080/01431160902897833.

- Stukel, M.R., Landry, M.R., Benitez-Nelson, C.R., and Goericke, R. 2011. Trophic cycling and carbon export relationships in the California Current Ecosystem. *Limnol. Oceanogr. Methods*, 56, 1866-1878.
- Subramanian, S.G.B., Sreekanth, N., Manjulekshmi, N., Singh, N.P., Kolwalkar, J., Patil, T., Fernandes, P.M., 2014. Manual on The use of Potential Fishing Zone (PFZ) forecast, Technical Bulletin No. 40, ICAR Research Complex for Goa (Indian Council of Agricultural Research), India.
- Suykens, K., Delille, B., Chou, L., De Bodt, C., Harlay, J., Borges, A.V., 2010. Dissolved inorganic carbon dynamics and air-sea carbon dioxide fluxes during coccolithophore blooms in the northwest European continental margin (northern Bay of Biscay), *Global Biogeochem. Cycles* 24, <http://dx.doi.org/10.1029/2009GB03730>.
- Vijith, V., Vinayachandran, P.N., Thushara, V., Amol, P., Shankar, D., Anil, A.C., 2016. Consequences of inhibition of mixed-layer deepening by the West India Coastal Current for winter phytoplankton bloom in the northeastern Arabian Sea, *J. Geophys. Res.*, doi:10.1002/2016JC012004.
- Vipin, P., Sarkar, K., Aparna, S.G., Shankar, D., Sarma, V.V.S.S., Gracias, D.G., Krishna, M.S., Srikanth, G., Mandal, B., Rama Rao, E.P., and Srinivasa Rao, N., 2015. Evolution and sub-surface characteristics of an SST Filament and Front in the Northeastern Arabian Sea during November-December 2012. *J. Mar. Syst.* 150, 1-11.
- Taylor, J.R., Ferrari, R., 2011. Ocean fronts trigger high latitude phytoplankton blooms. *Geophys. Res. Letters*. 38, doi: 10.1029/2011GL049312.
- Traganza, E.D., Redalje, D.G., and Garwood, R.W., 1987. Chemical flux, mixed layer entrainment and phytoplankton blooms at upwelling fronts in the California coastal zone. *Cont. Shelf Res.* 7, 89-105.
- Ullman, D.S., Cornillon, P.C., 2000. Evaluation of front detection methods for satellite-derived SST data using in situ observations. *Journal of Atmospheric and Oceanic Technology* 17 (12), 1667–1675.
- Videau, C. 1987. Primary production and physiological state of phytoplankton at the Ushant tidal front (west coast of Brittany, France). *Mar. Ecol. Prog. Ser.* 35, 141-151.
- Wiggert, J.D., Murtugudde, R.G., McClain, C.R. 2002. Processes controlling interannual variations in wintertime (northeast monsoon) biomass in the central Arabian Sea. *Deep Sea Res Part II*, 49, 2319–2343
- Wyrtki K (1971) *Oceanographic atlas of the International Indian Ocean Expedition*. National Science Foundation, Washington, DC, 531 pp
- Woodson, C.B., McManus, M.A., 2007. Foraging behavior can influence dispersal of marine organisms. *Limnol. Oceanogr.* 562, 2701-2709.
- Yoder, J.A., Ackleson, S.G., Barber, R., et al. 1994. A line in the sea. *Nature* 371, 689-692.
- Zhao, B.R. 1985. The fronts of the Huanghai Sea cold water mass induced by tidal mixing. *Chinese J. Oceanol. Limnol.*, 16, 451-459.

Table 1: Hydrographical properties in the frontal and non-frontal (NF) regions during Cruise #SSK-060 in the northeastern Arabian Sea. The values for the frontal and non-frontal region were averaged over the frontal and non-frontal stations, respectively, on each transect. Chl-*a*, NO₃, PO₄, SiO₄, POC (particulate organic carbon), PN (particulate nitrogen), PP (primary productivity), zooplankton biomass, and TBC (total bacterial count) are integrated over the top 50 m, while temperature, Fv/Fm, and C/N are averaged over this depth range. Frontal values are shown in italics merely to make it easier to follow the variation. Fronts T1 and T2 are in the open ocean (arranged south to north in the NEAS), Front T3 in the transition zone and Fronts T4 and T5 are over the shelf (offshore to inshore). TM (transect mean) denotes the average concentration estimated using the data from all stations on a transect; Tm is used to represent the background conditions in this paper. The climatological mean (CM) of each variable in the study region was estimated by averaging the data for all five transects; the CM value is given in parentheses in the first column.

		Front T1	Front T2	Front T3	Front T4	Front T5
Sea surface temperature (SST; °C) (25.02)	NF	25.36	25.09	24.83	25.33	25.20
	<i>Front</i>	<i>24.91</i>	<i>23.86</i>	<i>24.75</i>	<i>24.95</i>	<i>24.88</i>
	TM	25.17	24.78	24.77	25.19	25.04
Temperature (°C) (24.88)	NF	25.22	25.04	24.66	25.02	24.92
	<i>Front</i>	<i>24.81</i>	<i>23.83</i>	<i>24.41</i>	<i>24.56</i>	<i>24.45</i>
	TM	25.05	24.74	24.61	24.96	24.91
Chl- <i>a</i> (mg m ⁻²) (31.5)	NF	30.0	26.6	28.2	29.4	34.8
	<i>Front</i>	<i>28.3</i>	<i>60.1</i>	<i>36.2</i>	<i>31.3</i>	<i>44.1</i>
	TM	29.9	35.2	32.1	30.0	38.9
NO ₃ (mmol m ⁻²) (135.4)	NF	111.6	142.8	95.0	146.6	126.6
	<i>Front</i>	<i>118.3</i>	<i>190.8</i>	<i>125.0</i>	<i>173.6</i>	<i>135.1</i>
	TM	114.6	154.8	115.3	155.6	131.9
PO ₄ (mmol m ⁻²) (52.1)	NF	54.7	60.5	32.3	50.1	44.8
	<i>Front</i>	<i>55.0</i>	<i>70.9</i>	<i>49.6</i>	<i>54.3</i>	<i>47.3</i>
	TM	54.8	63.0	42.0	51.6	46.0
SiO ₄ (mmol m ⁻²) (148.7)	NF	100.3	117.0	132.7	134.3	125.6
	<i>Front</i>	<i>108.4</i>	<i>198.0</i>	<i>142.3</i>	<i>167.4</i>	<i>165.3</i>
	TM	104.0	137.2	139.2	145.4	145.5
Fv/Fm (0.44)	NF	0.43	0.44	0.44	0.38	0.46
	<i>Front</i>	<i>0.45</i>	<i>0.45</i>	<i>0.44</i>	<i>0.43</i>	<i>0.49</i>
	TM	0.44	0.44	0.44	0.40	0.47
POC (mg m ⁻²) (5309)	NF	5239	5132	4199	5168	6144
	<i>Front</i>	<i>5616</i>	<i>5127</i>	<i>5378</i>	<i>4931</i>	<i>6591</i>
	TM	5400	5130	4598	5089	6368

PN (mg m ⁻²) (1209)	NF	898	1191	1340	1336	1323
	<i>Front</i>	<i>1020</i>	<i>1014</i>	<i>1312</i>	<i>1297</i>	<i>1222</i>
	TM	950	1146	1321	1323	1273
C/N (5.8)	NF	7.4	5.0	4.7	5.3	6.4
	<i>Front</i>	<i>7.6</i>	<i>6.8</i>	<i>4.9</i>	<i>5.1</i>	<i>5.4</i>
	TM	7.5	5.4	4.8	5.2	5.9
PP (mgC m ⁻² d ⁻¹) (1172)	NF	681	862	486	743	2781
	<i>Front</i>	<i>781</i>	<i>620</i>	<i>564</i>	<i>1755</i>	<i>2427</i>
	TM	702	719	524	921	2532
Zooplankton biomass (mg m ⁻²) (1828)	NF	324	479	1181	813	1520
	<i>Front</i>	<i>597</i>	<i>906</i>	<i>1201</i>	<i>2176</i>	<i>1867</i>
	TM	427	586	1194	1540	1659
TBC (x 10 ⁸ Nos/L) (1.17)	NF	0.73	1.17	1.04	0.68	1.90
	<i>Front</i>	<i>1.26</i>	<i>4.08</i>	<i>1.28</i>	<i>1.00</i>	<i>1.13</i>
	TM	1.04	1.89	1.14	0.75	1.51

Table 2: Dates of formation and ending of fronts. The last column gives the approximate age in days at the time of sampling. The start and end times (IST: UTC+0530) are based on the satellite pass. Fronts T3A and T4A are the same filaments sampled on different dates.

Transect	Front	Start date	End date	Age at sampling time (days)
T1	T1A	22-Jan-2014 15:51	29-Jan-2014 09:33	3.3
	T1B	22-Jan-2014 10:27	26-Jan-2014 02:07	NA
T2	T2A	18-Jan-2014 10:00	24-Jan-2014 13:43	NA
	T2B	18-Jan-2014 10:00	25-Jan-2014 09:16	6
T3	T3A	18-Jan-2014 10:00	30-Jan-2014 01:26	11
	T3B	28-Jan-2014 21:03	30-Jan-2014 22:20	1.5
T4	T4A	18-Jan-2014 10:00	30-Jan-2014 01:26	9
	T4B	22-Jan-2014 15:51	30-Jan-2014 16:01	6
T5	T5A	28-Jan-2014 21:03	31-Jan-2014 01:15	0.5

Figure captions

Figure 1: Map showing the region of interest (upper left panel). The box marked in this panel shows the location of the region surveyed, a part of the northeastern Arabian Sea (NEAS) and is the domain used for the other three panels. The upper right panel shows the climatological mixed-layer depth (MLD; m) for January; the temperature and salinity data are from the climatology of Chatterjee et al. (2012). The MLD was estimated as the depth at which the density increase from the surface corresponds to a 1.0 °C decrease in temperature (Shenoi et al., 2004; Shankar et al., 2015). The lower left panel shows the SST (°C) during the sampling period (24-30 January 2014). Since the SST contoured is an average over a few days, the fronts are not marked in this figure; instead, they are shown in Figures 2-6, which describe the individual transects. The minimum, mean and maximum SST averaged over the domain and this week were 21.22°C, 24.86 °C and 26.79 °C respectively. The lower right panel shows the weekly climatology of Chl-a for the week centred on 29 January; the data are from Lévy et al. (2006). In the panels for MLD, SST, and Chl-a, the transects sampled are shown by the black lines and the sampling stations by the black squares. The labels indicate the first and last stations on each transect: for example, T1a and T1j indicate the first and last stations on Transect 1. Note that the first station is not at an end of the transect for Transect 2. Also marked on this map are the PFZ curves as per the advisories issued by INCOIS; a different colour is used for each of the days during 25-30 January. The shelf break (200 m isobath) is shown by the black dashed curve.

Figure 2: Remote-sensing and in situ data for Transect 1 (T1). The panels at the top on the left show SST (colour, °C), with the SST fronts superimposed on them. The transect is shown blue line and the sampling stations are marked by the filled blue circles. The panels at the bottom on the left show the evolution of fronts T1A and T1B. The black (red) curve marks the beginning (end) of the front. The grey (pink) curves show the front before (after) the sampling period. The curves in other colours show the front at specific times during the sampling of the transect; the time of the satellite pass is given below the last panel on the left. In all the panels on the left, the 200 m isobath is shown by the black dashed curve. The evolution of Front T1A is superimposed on SST maps in Fig. S2. The panels on the right show the in situ data collected along the transect; distance, on the abscissa, is measured along the transect from northwest (left) to southeast (right). The variables plotted, from top to bottom, are temperature (°C), Chlorophyll-a (mg m^{-3}), nitrate (μM), phosphate (μM), silicate (μM), and particulate organic carbon (μM). The date and time of the sampling is given at the top of the first panel and the station number is given at the bottom of each panel. The number in parentheses following the station number is the MLD (m). The MLD for all stations is shown in Figure S1. The name of the front and the time of sampling are coloured red. The averaged, vertically integrated values for all these frontal stations are listed under “front” in Table 1, and the averaged, vertically integrated values of the other (non-frontal) stations (sampling time coloured black) are listed under “non-frontal” (NF) regime.

Figure 3: Same as Figure 2, but along Transect 2 (T2). The distance is computed from northwest to southeast, but note that this transect was not sampled in order along the line shown: the first station sampled was T2a, where front T2B was located at that time, followed by station T2b, which was at the northwestern end of the transect. The evolution of Front T2B is superimposed on SST maps in Figure S2.

Figure 4: Same as Figure 2, but along Transect 3 (T3). The distance is computed from west to east, but this transect was sampled in the opposite direction and the time therefore increases from right to

left in the panels on the right. The evolution of Front T3A (T3B) is superimposed on SST maps in Figure S3 (S4).

Figure 5: Same as Figure 2, but along Transect 4 (T4). The distance is computed from west to east. The evolution of Front T4A (T4B) is superimposed on SST maps in Figure S3 (S5). The ML extended to the bottom at stations T4f, T4g, and T4h.

Figure 6: Same as Figure 2, but along Transect 5 (T5). The distance is computed from west to east, but this transect was sampled in the opposite direction and the time therefore increases from right to left in the panels on the right. The evolution of Front T5A is superimposed on SST maps in Figure S6. The ML extended to the bottom at all stations on this transect.

Figure 7: Typical distribution of temperature, Chlorophyll-a, nitrate, and TBC in the frontal and NF regimes in the open ocean (top panel) and on the shelf (bottom panel). The fitted lines drawn are for the frontal (solid curve) and non-frontal (dashed curve) regimes.

Figure 8: Schematic representation of the biological response in the shelf and open-ocean fronts. OM: organic matter.

Figure 9: Schematic representations of biological responses in the fronts sampled.

Figure 1

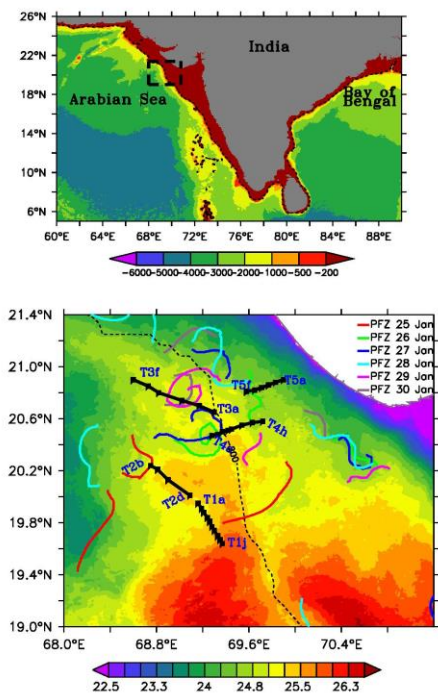


Figure 2

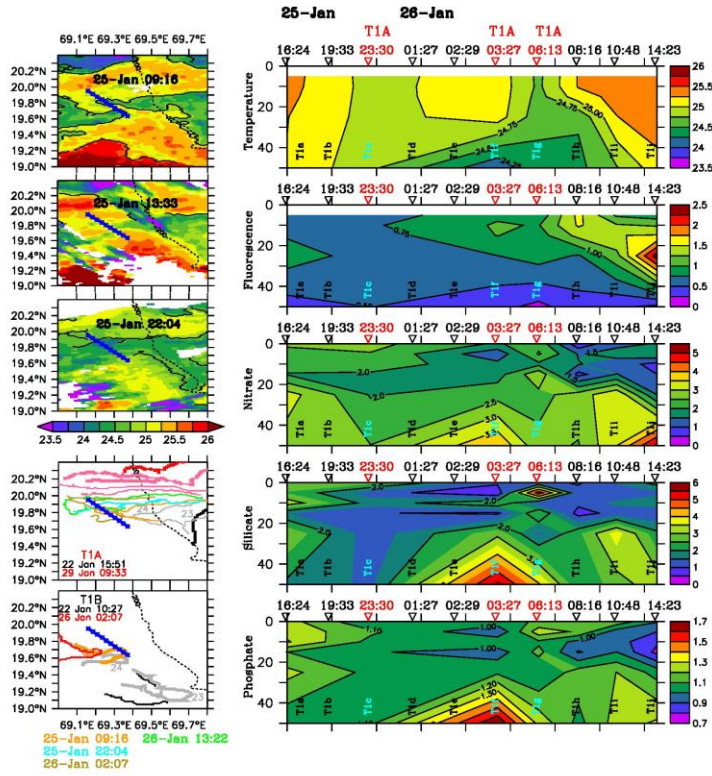


Figure 3

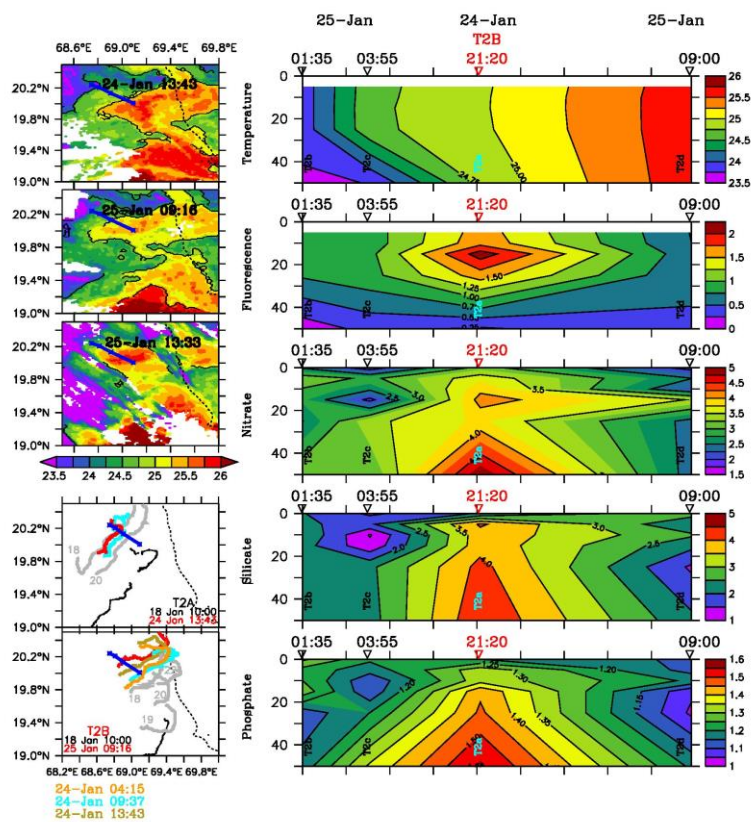


Figure 4

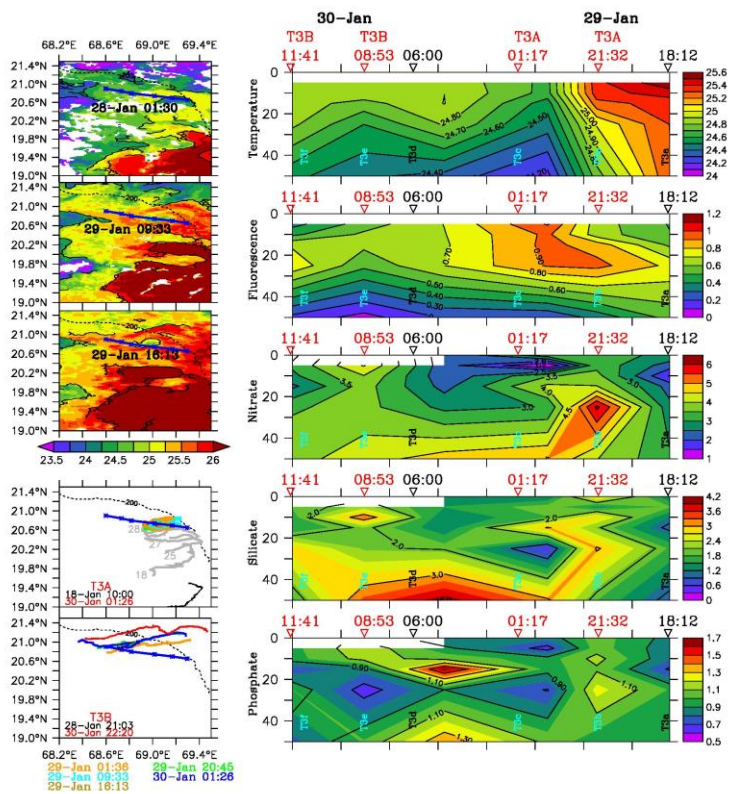


Figure 5

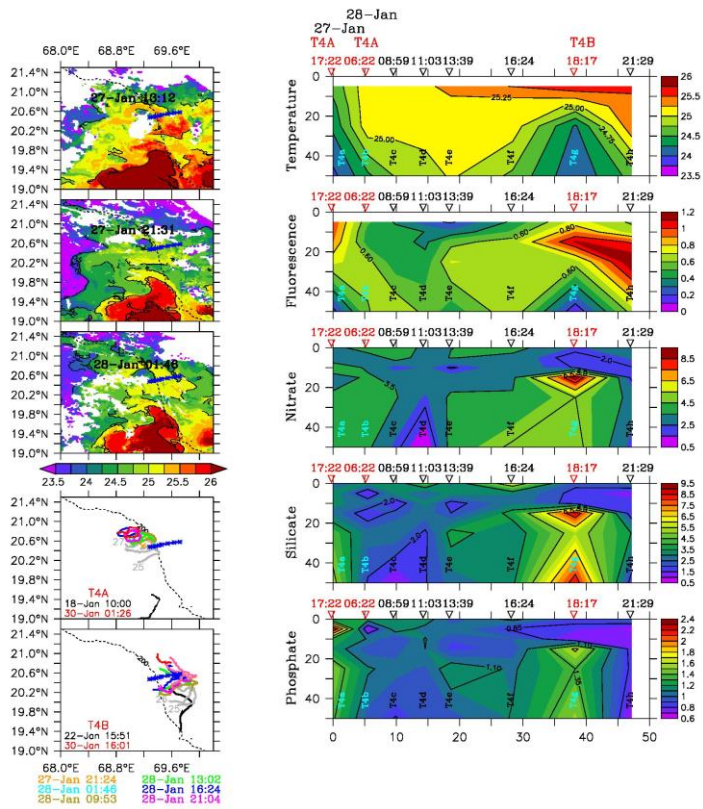


Figure 6

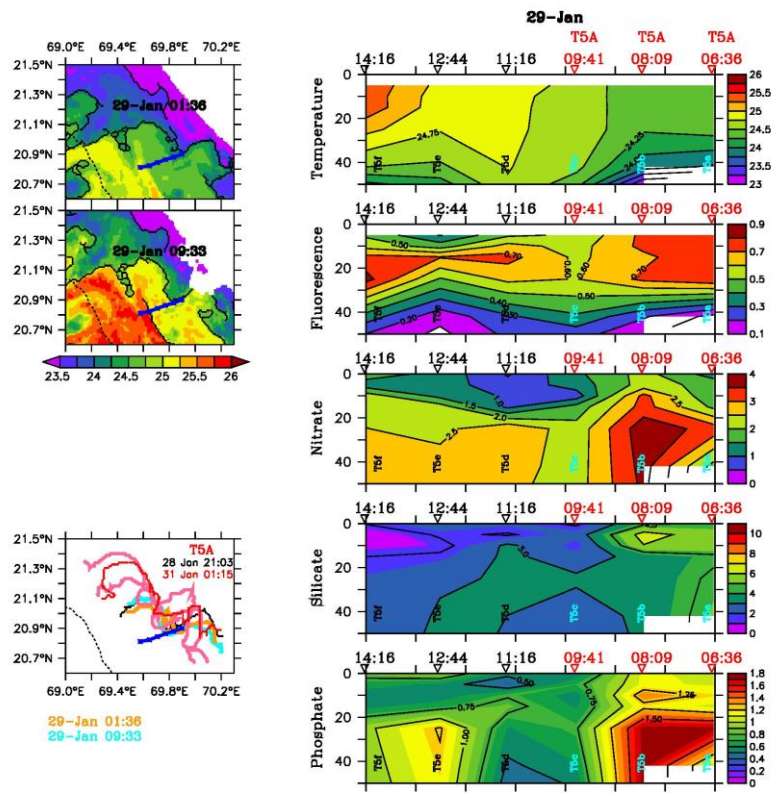


Figure 7

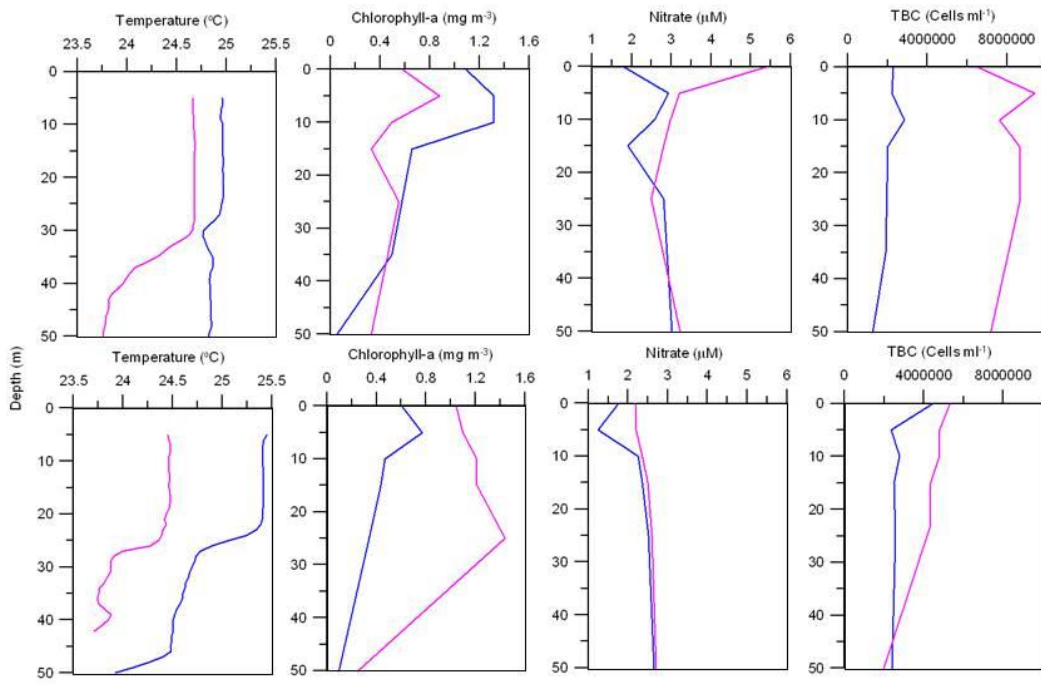


Figure 8

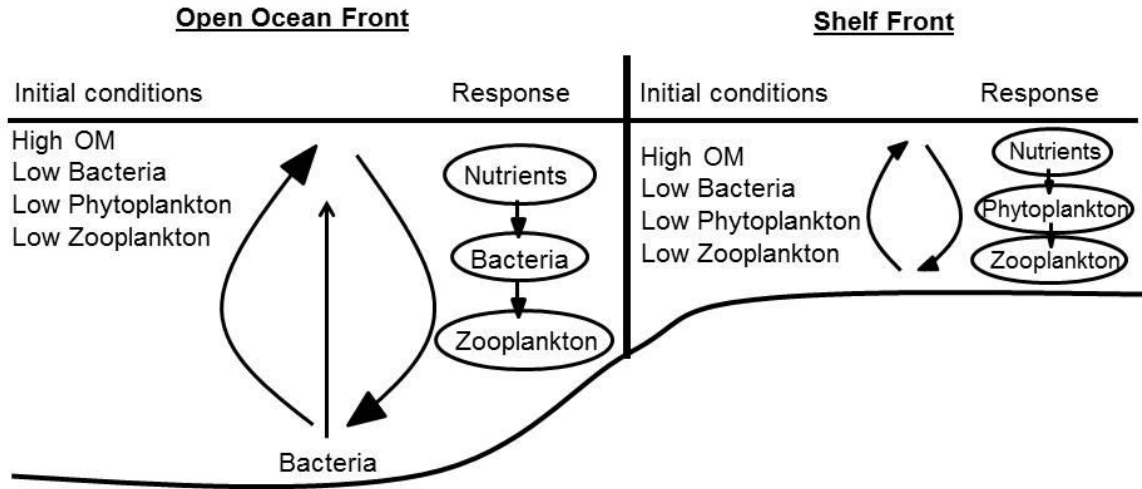


Figure 9

